atmosphere

MDPI

Article

Vertical Structure and Dynamical Regimes of Mediterranean Tropical-like Cyclones from High-Resolution WRF Simulations

Christian Natale Gencarelli [1,*] and Francesco Carbone [2,*]

[1] National Research Council, Institute of Environmental Geology and Geoengineering, 20131 Milan, Italy
[2] National Research Council, Institute of Atmospheric Pollution Research, 87036 Rende, Italy
* Correspondence: christiannatale.gencarelli@cnr.it (C.N.G.); francesco.carbone@cnr.it (F.C.)

Abstract

Mediterranean tropical-like cyclones (MTLCs), commonly referred to as Medicanes, are high-impact weather systems characterized by complex interactions between baroclinic forcing and tropical-like processes. Despite growing interest, their vertical structures and dynamical regimes remain incompletely understood. In this study, high-resolution Weather Research and Forecasting (WRF) simulations at 1 km resolution are used to investigate the structure and evolution of two dynamically contrasting MTLCs: Ianos (2020) and Qendresa (2014). The analysis focuses on the temporal evolution of kinetic energy and turbulent dissipation as well as on the three-dimensional organization of wind and temperature fields during representative phases of the cyclone life cycle. The results reveal pronounced differences between the two events, with Ianos exhibiting a compact, vertically coherent, convection-dominated structure and Qendresa showing a wider, more asymmetric, and less stationary organization influenced by baroclinic processes. A comparative framework with the ERA5 reanalysis is employed to contextualize cyclone intensity, with ERA5 used as a dynamically consistent large-scale reference rather than as an observational benchmark. Overall, the study highlights the importance of vertical structure and boundary-layer processes in shaping Mediterranean tropical-like cyclones and demonstrates the added value of high-resolution numerical simulations for distinguishing between different dynamical regimes.

Keywords: Medicane; WRF; cyclones

1. Introduction

Tropical cyclonic systems are among the most severe atmospheric phenomena worldwide. Although they are typically associated with tropical latitudes, cyclones exhibiting tropical-like characteristics have also been documented in mid-latitude regions. In the Mediterranean basin, these phenomena are referred to as Mediterranean Tropical-Like Cyclones (MTLCs), or Medicanes, and can produce intense winds, heavy precipitation, and severe marine conditions [1–3]. These events account for a large fraction of extreme wind occurrences in the region and are frequently associated with hazardous sea states, posing substantial risks to densely populated and highly vulnerable coastal areas [4–6].

Tropical cyclones typically form over warm and relatively homogeneous oceanic environments, whereas MTLCs develop within a semi-enclosed basin characterized by strong land–sea thermal contrasts, complex orography, and pronounced horizontal gradients of temperature and moisture. Their evolution is controlled by the combined influence of mid-latitude dynamical mechanisms, such as upper-level potential vorticity anomalies

Academic Editor: Michael L. Kaplan

Received: 16 February 2026
Revised: 9 March 2026
Accepted: 19 March 2026
Published: 21 March 2026

and baroclinic instability, and tropical-like processes including moist convection, surface heat fluxes, and the establishment of a symmetric warm core [7]. This combination of processes gives rise to a broad spectrum of structural and dynamical configurations, which complicates both the classification and the prediction of MTLCs.

The Mediterranean region has been identified as a climate-change hotspot [8,9], exhibiting warming rates that exceed the global average. Increasing sea surface temperatures (SSTs) and enhanced atmospheric instability have been discussed as factors that may contribute to conditions favorable for the development of more intense MTLCs [10,11]. Nevertheless, quantifying the response of these systems to climate forcing remains challenging due to the limited number of documented events, the relatively short observational record, and their strong dependence on the large-scale environmental setting [2,3]. These aspects complicate both the physical interpretation of MTLC dynamics and the development of reliable forecasting strategies.

High-resolution numerical modeling has become increasingly important for the investigation of MTLCs, as it enables the evolution and internal structure of these systems to be examined in a dynamically consistent manner [12,13]. Within the constrained Mediterranean basin, mesoscale and thermodynamic processes play a decisive role once cyclogenesis is initiated [12,14]. In particular, the interaction between convective development, latent heat release, and planetary boundary layer (PBL) processes exerts a strong control on cyclone intensity and structure [15]. Upper-tropospheric potential vorticity intrusions associated with Rossby wave breaking are frequently associated with the presence of strong baroclinic forcing and contribute to shaping the synoptic environment conducive to MTLC development [13]. The interaction between these large-scale circulation features and embedded convection further modulates moisture transport, precipitation patterns, and wind impacts [12,16].

Despite substantial progress in numerical modeling and case-study analyses, several fundamental aspects of MTLC dynamics remain insufficiently explored. In particular, the vertical organization of these systems and the role of the PBL in mediating the coupling between surface forcing and free-tropospheric dynamics have not yet been addressed in a systematic way, as also highlighted in Flaounas et al. [13]. This gap limits the ability to interpret how different dynamical pathways can lead to similar tropical-like structures and how surface-driven processes contribute to the three-dimensional organization of MTLCs.

Recently, atmospheric reanalyses have been increasingly adopted as dynamically consistent large-scale references for the evaluation and intercomparison of high-resolution regional simulations over the Mediterranean [2,13]. In particular, ERA5 has been widely used to assess relative differences in moisture transport, cyclone-related variables, and extreme events simulated by regional models, without interpreting the reanalysis as a direct observational benchmark [17–19]. Within this context, ERA5 provides a coherent large-scale background against which convection-permitting simulations, characterized by horizontal grid spacings fine enough to explicitly resolve deep convection without the use of cumulus parameterization, can be compared in terms of cyclone intensity, structure, and temporal evolution. Following this approach, ERA5 is used in the present study exclusively as a reference dataset to support a comparative assessment of Weather Research and Forecasting (WRF) simulations.

In fact, the present study adopts a physically interpretable, model-based perspective to investigate MTLC dynamics using convection-permitting simulations performed using the WRF model [20]. The analysis focuses on the vertical structure and evolution of two dynamically contrasting MTLCs: Ianos (September 2020), a strongly convective system characterized by a well-defined warm core [15], and Qendresa (November 2014), which developed through a subtropical transition from an extratropical precursor [13]. These

two cases were selected because they represent distinct dynamical pathways leading to tropical-like cyclones within the Mediterranean basin.

Comparing these events within a unified high-resolution modeling framework, the study aims to clarify how PBL processes, vertical stratification, and large-scale environmental conditions shape MTLC structure and evolution. Rather than focusing on model performance, the analysis emphasizes the physical organization of MTLCs. The novelty of this work lies not only in the combined analysis of energetic diagnostics and three-dimensional cyclone structure but also in the use of a unified convection-permitting modeling framework to compare two dynamically contrasting MTLCs under multiple physically plausible parameterization settings. This approach makes it possible to assess which structural and energetic features are robust across model configurations and which are regime-dependent, thereby providing a physically grounded perspective on the dynamical diversity of MTLCs and on the role of PBL and surface-driven processes in shaping their evolution.

This work is organized as follows: Section 2 describes the case studies, the WRF model configuration, and the adopted physical parameterizations, as well as the comparative framework with ERA5; Section 3 presents the results of the numerical simulations and their analysis; Section 4 discusses the main findings from a modeling perspective; finally, Section 5 summarizes the main conclusions of the study.

2. Materials and Methods

2.1. Case Studies

In this study, a focus is placed on two MTLCs, which offer a valuable opportunity to investigate the diversity and complexity of tropical-like cyclones in the Mediterranean basin. The Medicane Ianos (September 2020) and Qendresa (November 2014) are analyzed as representative case studies, as they revealed distinct mechanisms of development and intensification, while also producing significant socioeconomic impacts.

The Medicane Ianos was selected for its notable intensity and tropical-like characteristics, which were developed under conditions of high SST (Figure 1) that fueled intense convection and a well-defined eye, typical of tropical cyclones. Its strength, which is comparable to a Category 1 hurricane on the Saffir-Simpson scale with winds up to 150 km h^{-1}, makes Ianos one of the most intense events ever recorded in the Mediterranean Sea [21]. The severe impacts associated with Ianos, including strong winds, heavy rainfall, and storm surges, fueled a broader debate on the increasing frequency and intensity of Mediterranean tropical-like cyclones and their possible link to climate change and Mediterranean Sea surface warming. These impacts further highlighted the need to improve early warning systems and emergency management strategies in the Mediterranean region. The crucial role of convective parameterization and the interplay between upper-level baroclinic dynamics and surface processes has been underscored by several sensitivity studies [7,22].

The Medicane Qendresa is an exemplary case of a system that underwent a clear subtropical transition after initially developing as an extratropical cyclone. This characteristic has contributed to research on the formation and evolution of hybrid systems and has helped improve the understanding of their dynamics. The deepening and tropical transition of Qendresa were attributed to the synergistic effect of baroclinic and diabatic processes, with strong control over the system's intensity being exerted by SST. In this case, a secondary role appeared to be played by wind induced surface heat exchange mechanisms. The Medicane Qendresa was developed within the broader circulation of a synoptic-scale system and its evolution was influenced by its interaction with an upper-level potential vorticity streamer. Together with other Mediterranean cyclones such as Numa and Zorbas, the severe impacts associated with Qendresa made it a fundamental

case study for meteorologists, providing valuable data for the analysis and prediction of future events [13].

The Qendresa simulation was initialized on 4 November 2014 and ran until 10 November 2014, while for the Ianos case study the model integration began on 14 September 2020 and ended on 20 September 2020. The adopted configuration ensured consistency with the large-scale atmospheric forcing and, through the use of nested high-resolution domains, allowed the simulation of the mesoscale and fine-scale dynamics involved in the cyclone life cycle and intensification.

The variety of their life cycles, their interaction mechanisms with the surrounding environment, and their spectral characteristics can be examined through the comparative analysis of these two events, thereby providing a more profound understanding of the complex dynamics that govern them.

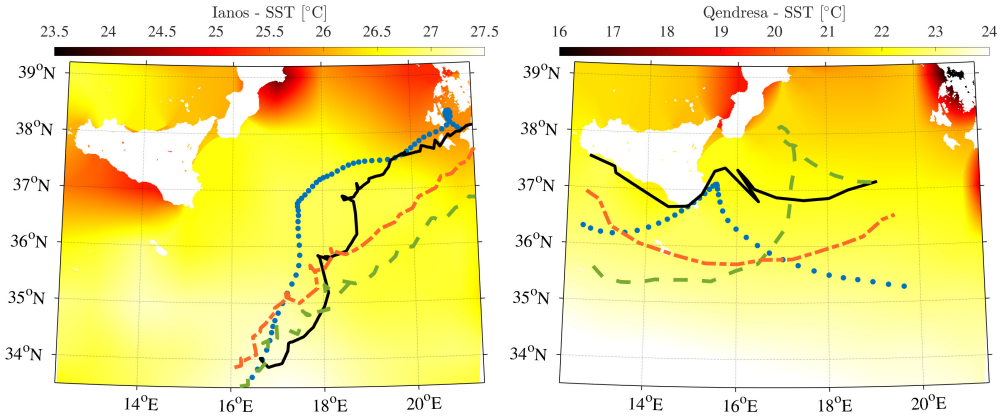

Figure 1. WRF SST fields for Medicane Ianos (**left** panel) and Medicane Qendresa (**right** panel). Superimposed are the reference track (blue, Flaounas et al. [23]) and simulated optimal tracks from three WRF experiments: S01 (black), S02 (red), and S03 (green).

2.2. Weather Research and Forecasting Model Setup

The numerical simulations of the selected Medicanes were performed using the Weather Research and Forecasting (WRF) regional atmospheric model, version 4.3.3 [20]. The WRF model was selected because of its capability to explicitly represent mesoscale and sub-mesoscale processes through the use of nested domains at high spatial resolution and advanced numerical formulations, which are required to properly simulate the complex dynamics of MTLCs. The dynamical core employs a third-order Runge-Kutta time integration scheme together with sixth-order advection schemes in the horizontal and vertical directions, ensuring numerical accuracy and stability.

The model setup consisted of three two-way nested domains (Figure 2), sharing a common vertical discretization of 49 levels extending from the surface to 50 hPa. The outermost domain, with a horizontal grid spacing of 25 km, encompasses Europe and the Mediterranean region, including portions of North Africa and the Middle East. An intermediate domain with 5 km horizontal resolution was nested within the coarse grid, covering the entire Mediterranean basin and a substantial part of Europe. The innermost domain, characterized by a horizontal resolution of 1 km $\times$ 1 km, was centered over the area affected by the investigated MTLCs to resolve fine-scale structures. This discretization represents a compromise between computational cost and the need to adequately resolve boundary-layer and lower-tropospheric processes relevant to MTLC dynamics.

Initial and lateral boundary conditions were provided by the National Centers for Environmental Prediction (NCEP) Final Analysis (FNL) dataset [24], available at 1° $\times$ 1° horizontal resolution and 6-hourly temporal frequency. No nudging was applied during

the simulations to allow the model to freely evolve the mesoscale features of the investigated MTLCs.

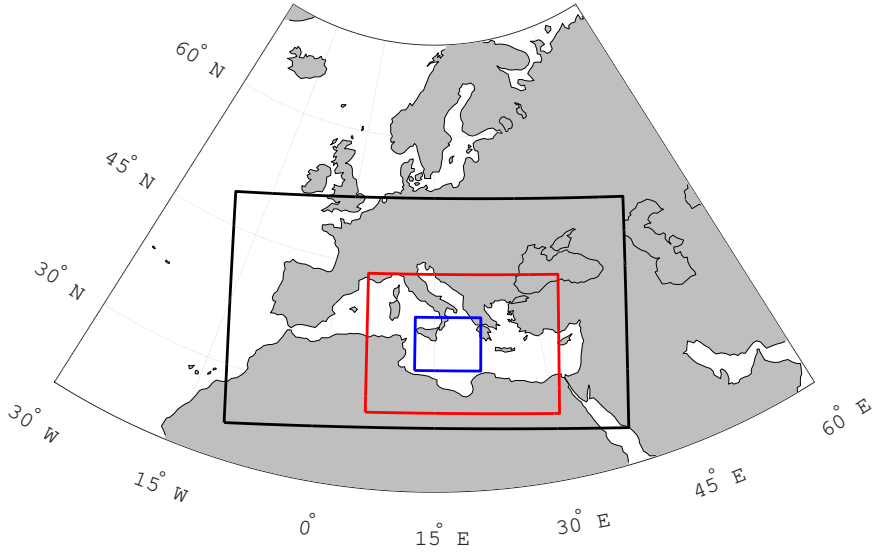

Figure 2. WRF model domains: black box for coarse domain (25 km), red box for middle domain (5 km), and blue box for fine domain (1 km), where the analysis of MTLC structure is performed.

To identify the periods characterized by a quasi-stationary flow regime, the domain-averaged turbulent kinetic energy (TKE) $E_k(t)$ and the TKE dissipation rate $\epsilon(t)$ were analyzed as physical proxies. These variables were diagnosed directly from the WRF model output: E_k is calculated from the resolved velocity components, while ϵ is derived following the model's internal formulation consistent with the selected PBL scheme. This diagnostic approach ensures that the stationarity of the flow is assessed based on the balance between energy production and dissipation within the simulated atmospheric volume.

In line with turbulence theory, the stabilization of E_k and ϵ serves as a diagnostic for the cyclone's mature phase. The quasi-stationarity indicates that the vortex has reached a structural equilibrium where the turbulent energy budget is no longer dominated by rapid intensification transients.

TKE was estimated diagnostically using scaling relationships based on friction velocity and atmospheric stability, which are commonly used to characterize turbulence intensity in the atmospheric boundary layer [25–27]. The vertical stability was first quantified through the Brunt–Väisälä frequency,

$$N^2 = \frac{g}{\theta}\frac{\partial \theta}{\partial z}, \tag{1}$$

where g is the gravitational acceleration, θ is the potential temperature, and $\partial\theta/\partial z$ is the vertical gradient of potential temperature.

Using the friction velocity u_* provided by the WRF output, the TKE was then estimated as

$$E_k = C_k \frac{u_*^2}{\sqrt{N^2}}, \tag{2}$$

where $C_k = 0.2$ is an empirical coefficient.

The dissipation rate was estimated using the classical turbulence scaling

$$\epsilon = \frac{E_k^{3/2}}{\kappa z}, \tag{3}$$

where κ is the von Kármán constant and z represents the height above ground level. The height z was obtained from the base-state geopotential Φ and perturbation of the geopotential Φ_{pert} as

$$z = \frac{\Phi + \Phi_{\text{pert}}}{g}. \quad (4)$$

This approach allows for a physically consistent evaluation of the energy budget and the scaling properties of the boundary layer, assuming a characteristic mixing length proportional to height above ground [28].

2.3. Physical Parameterizations

Three WRF simulation configurations, hereafter referred to as S01, S02, and S03, were designed to investigate the sensitivity of MTLCs to different physical parameterization combinations. The selection of parameterization schemes was guided by previous sensitivity studies focusing on MTLCs and similar mesoscale systems [7,22].

In configuration S01, the Thompson microphysics scheme was adopted for its detailed representation of mixed-phase hydrometeors, enabling a realistic simulation of cloud and precipitation processes. The Yonsei University (YSU) PBL scheme was used to represent vertical mixing, atmospheric stability, and near-surface meteorological variables relevant to cyclone PBL dynamics. The Eta surface layer and the Noah land surface model were also implemented. Longwave and shortwave radiative transfer were parameterized using the rapid radiative transfer model (RRTM) and Dudhia schemes, respectively. The Kain-Fritsch cumulus parameterization was applied only to the two outer domains (25 km and 5 km), while convection was explicitly resolved in the innermost domain (1 km resolution), consistent with its fine spatial scale.

In configuration S02, the physical setup was identical to S01, except for the use of the simpler Kessler microphysics scheme, allowing the role of microphysical complexity to be examined in isolation. In configuration S03, the Kessler microphysics scheme was again employed, while both shortwave and longwave radiation were parameterized using the community atmosphere model (CAM) scheme. The CAM radiation scheme provides a more detailed representation of cloud-radiation interactions and atmospheric gas absorption, whereas the Dudhia and RRTM schemes prioritize computational efficiency and a physically based treatment of shortwave and longwave radiative processes, respectively.

The combination of these three configurations is designed to test the robustness of the simulated MTLC structure and energetics across physically plausible representations of microphysical and radiative processes. The objective is not to identify a single optimal setup, but to determine whether the inferred dynamical regime of each cyclone remains stable under changes in parameterized physics. In this sense, the analysis does not merely compare configurations, but uses configuration diversity as a tool to separate robust physical signals from setup-dependent variability. The objective is not to quantify parameter sensitivity in a statistical sense, but rather to assess the robustness of the identified dynamical regimes across physically plausible model configurations. Table 1 summarizes the physical parameterizations adopted in the three simulations.

Table 1. Summary of physical parameterization schemes adopted in the three WRF simulations. The Kain–Fritsch cumulus parameterization is applied only in the outer domains with 25 km and 5 km resolution. A dash (–) indicates that the same option as in simulation S01 was used.

Scheme Type	S01	S02	S03
Microphysics	Thompson	Kessler	Kessler
LW Rad.	RRTM	–	CAM
SW Rad.	Dudhia	–	CAM

Table 1. *Cont.*

Scheme Type	S01	S02	S03
Cumulus	Kain–Fritsch	–	–
PBL	YSU	–	–
Surface Layer	Eta	–	–
Land Surface	Noah	–	–

2.4. WRF–ERA5 Comparison Methodology

To complement the analysis, a methodology for comparing the WRF simulations with the ERA5 reanalysis [29] was adopted. ERA5 is used as a dynamically consistent large-scale reference to quantify relative differences in cyclone intensity and near-surface wind fields, rather than as a surrogate for direct observations.

ERA5 is the fifth-generation global atmospheric reanalysis produced by the Copernicus Climate Change Service (C3S) at the European Centre for Medium-Range Weather Forecasts (ECMWF). It provides a physically and dynamically consistent reconstruction of the atmospheric state by combining a comprehensive set of in situ and remotely sensed observations with a state-of-the-art numerical weather prediction system through four-dimensional variational data assimilation [30]. The reanalysis is available at hourly temporal resolution on a regular latitude-longitude grid with a horizontal spacing of 0.25°. ERA5 includes a wide range of near-surface and upper-air variables, allowing for a coherent representation of large-scale circulation patterns and surface atmospheric conditions [29].

In this study, ERA5 single-level fields are employed exclusively as a large-scale reference for the comparison to the intensity and near-surface wind characteristics simulated by the high-resolution WRF configurations, without interpreting the reanalysis as a direct observational benchmark. The comparison is intentionally restricted to bulk intensity metrics, as the effective resolution of ERA5 does not allow for a reliable representation of the compact inner-core structure and associated vertical coherence resolved by high resolution simulations. Consequently, no direct structural comparison is attempted.

For each time step, minimum sea-level pressure (MSLP) and maximum 10 m wind speed (MWS) were extracted within a fixed-radius area centered on the cyclone core. This approach allows for a consistent comparison between datasets despite differences in spatial resolution and temporal sampling. To ensure physical consistency, the quantitative comparison was restricted to time steps in which the diagnosed cyclone center was located over marine grid points. Land-based phases were excluded from the statistical evaluation in order to avoid the influence of heterogeneous surface properties and orographic forcing, which are known to strongly affect cyclone structure and predictability over land [13].

To ensure a consistent spatial sampling of cyclone intensity across datasets with different horizontal resolutions, MSLP and MWS were extracted within a fixed-radius area centered on the cyclone core. A reference radius of 100 km was adopted, representing a compromise between capturing the core structure of the cyclone and minimizing the influence of the surrounding environmental flow, while remaining compatible with the effective resolution of the ERA5 reanalysis. Sensitivity tests using alternative radii of 50 km and 200 km did not reveal significant differences, indicating that the comparison is robust with respect to the choice of the diagnostic radius.

The statistical comparison is based on the mean bias (MB), root mean square error (RMSE), and mean absolute error (MAE), defined respectively as:

$$\mathrm{MB} = \frac{1}{N}\sum_{i=1}^{N}\left(X_i^{\mathrm{WRF}} - X_i^{\mathrm{ERA5}}\right), \tag{5}$$

$$\mathrm{RMSE} = \sqrt{\frac{1}{N}\sum_{i=1}^{N}\left(X_i^{\mathrm{WRF}} - X_i^{\mathrm{ERA5}}\right)^2}, \tag{6}$$

$$\mathrm{MAE} = \frac{1}{N}\sum_{i=1}^{N}\left|X_i^{\mathrm{WRF}} - X_i^{\mathrm{ERA5}}\right|. \tag{7}$$

3. Results

3.1. WRF-Simulated Cyclone Tracks

As a first step, the agreement between the simulated and observed cyclone positions was evaluated by comparing the distance between the modeled cyclone center and the corresponding reference track.

The observed reference tracks (hereafter referred to as Ref) were taken from the dataset of Flaounas et al. [23], which provides high-resolution reanalysis-based trajectories of Mediterranean cyclones.

The cyclone center in the WRF simulations was identified using CyTrack [31], an automated cyclone-tracking toolbox designed to follow tropical cyclones and Mediterranean tropical-like cyclones. The algorithm identifies candidate cyclone centers based on a combination of meteorological indicators, including MSLP and relative vorticity, and subsequently applies a spatio-temporal matching procedure to link cyclone features across successive time steps. This procedure allows for a consistent reconstruction of cyclone trajectories and their temporal evolution throughout the simulation period, providing the optimal track.

For the Medicane Ianos all simulations reproduce the general structure of the Ref trajectory, which initially moves northward toward southeastern Sicily, then curves eastward and southeastward. However, all simulated tracks exhibit a systematic southward displacement, especially in the northernmost segment. Configuration S01 (black) remains closest to the Ref path, particularly during the ascent and initial curvature, although it diverges earlier and advances more rapidly in the final southeastward stretch. S02 (blue) and S03 (red) follow similar patterns but remain consistently farther south. These differences highlight the sensitivity of cyclone propagation to physical parameterizations, especially in relation to orographic interaction and coastal proximity. For Medicane Qendresa, the simulations capture the general northward progression and eastward turn of the Ref track, but with larger deviations, particularly in the later stages. S01 again shows the best agreement, closely following the ascent and curvature near Sicily. S03 deviates more zonally and remains south and east of the Ref path, suggesting delayed intensification and weaker land interaction. S02 displays the highest variability, with premature poleward excursions and a final trajectory that remains displaced. These behaviors likely reflect differences in convective activity and instability linked to the parameterization schemes.

Using the cyclone center coordinates, spatial distances from the Ref track were computed at each time step. Table 2 summarizes the mean and standard deviation of these distances. For Medicane Ianos, S01 yields the lowest mean error (73.2 km), followed by S03 (110.4 km) and S02 (146.6 km), with relatively low variability across all configurations. For Medicane Qendresa, errors are larger and more variable: S01 again performs best (163.5 km), followed by S02 (172.9 km) and S03 (258.2 km), with standard deviations up to 119.7 km.

These results indicate differences in agreement with the reference track dataset across the different configurations. However, the markedly higher errors for Qendresa reflect its lower predictability, as noted in previous studies [32], which attributes this to limited marine observations and sensitivity to cumulus and microphysics schemes [33]. As a

baroclinic-to-tropical transition system, Qendresa exhibits greater dynamical instability and structural fragility compared to the more convectively driven Ianos.

Table 2. Mean distance ± standard deviation (km) between the Flaounas et al. [23] reference track (Ref) and each simulations configuration (S01, S02, S03).

Distance	Ianos	Qendresa
Ref-S01	73.2 ± 23.5	163.5 ± 119.7
Ref-S02	146.6 ± 53.2	172.9 ± 33.6
Ref-S03	110.4 ± 37.4	258.2 ± 94.5

3.2. Temporal Evolution of Energetic Diagnostics

To characterize the temporal evolution of the simulated cyclones and to identify dynamically representative phases, the TKE $E_k(t)$ and the TKE dissipation rate $\epsilon(t)$ were analyzed.

Figure 3 shows the temporal evolution of $E_k(t)$, normalized on the average domain kinetic energy $\langle E_\Omega \rangle$, and of $\epsilon(t)$, normalized on the average domain energy dissipation rate $\langle \epsilon_\Omega \rangle$, for the three simulation configurations (S01, S02, and S03). The temporal behavior differs substantially between the two case studies and across the different physical setups.

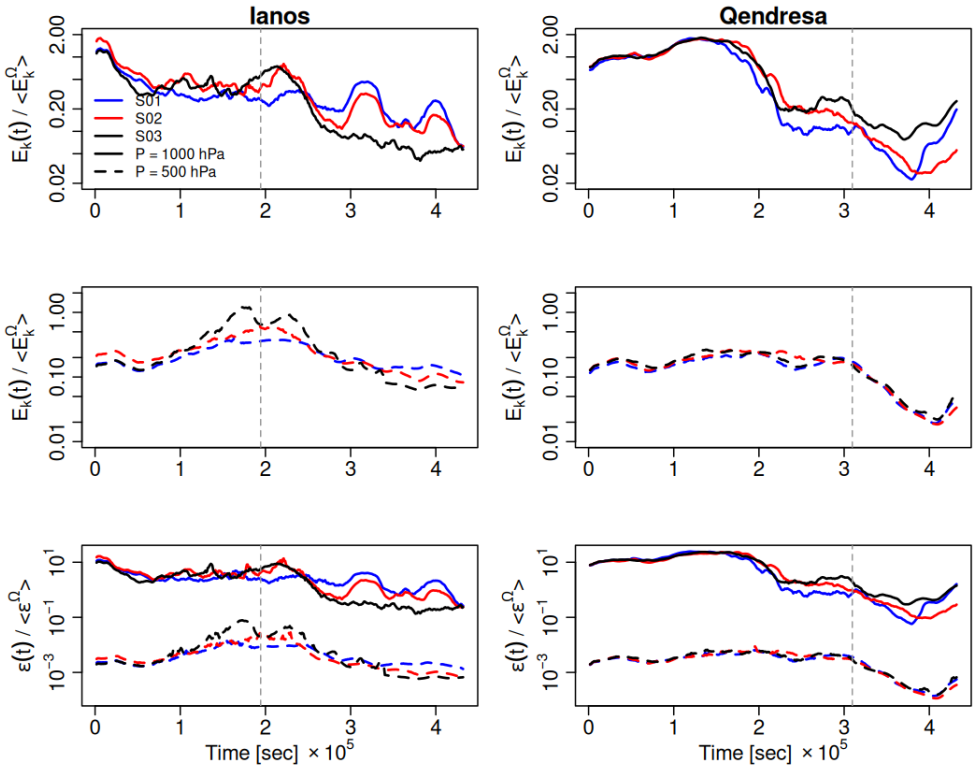

Figure 3. Temporal evolution of the TKE $E_k(t)$, normalized by the average domain kinetic energy $\langle E_\Omega \rangle$, for Ianos (**left** column) and Qendresa (**right** column). The upper and middle rows show $E_k(t)$ at 1000 hPa and 500 hPa, respectively. The lower row shows the temporal evolution of the TKE dissipation rate $\epsilon(t)$, normalized by the average domain dissipation rate $\langle \epsilon_\Omega \rangle$. Angle brackets denote temporal averaging. Vertical dashed lines indicate the reference times selected for the analysis of instantaneous fields discussed in the following Sections (17 September 2020 06:00 for Ianos and 8 November 2014 14:00 for Qendresa). All panels use a logarithmic scale on the y-axis.

For Ianos, all three configurations exhibit the establishment of a relatively well-defined mature phase, characterized by limited fluctuations around the mean values of $E_k(t)$ and $\epsilon(t)$. Configuration S01 shows a more regular behavior, with limited oscillations in both $E_k(t)$ and $\epsilon(t)$, whereas S02 and S03 display progressively larger temporal variability, particularly in $\epsilon(t)$.

The contrast between the two cyclones is robust across all configurations and suggests that the temporal behaviour of $E_k(t)$ and $\epsilon(t)$ provides a useful diagnostic of the underlying MTLC regime. In particular, the emergence of a quasi-stationary energetic state in Ianos and its significantly higher variability in Qendresa support the interpretation of the former as a more vertically coherent, convection-dominated vortex and of the latter as a less stationary system still strongly modulated by baroclinic forcing.

The selected reference times (vertical dashed lines in Figure 3) correspond to dynamically representative phases of the MTLC life cycle, as identified from the temporal evolution of $E_k(t)$ and $\epsilon(t)$. The time series confirms that the spatial structures discussed in the following sections are not sensitive to the exact timing of the selected snapshots. As an example, the WRF surface pressure anomalies, defined as $f(\mathbf{r}) - \langle f(\mathbf{r}) \rangle$ where $f(\mathbf{r})$ is a generic spatial variable and $\langle f(\mathbf{r}) \rangle$ is the average value of the variable at a fixed isobaric level, for the reference times are shown in Figure 4. For Ianos, the field corresponds to a fully mature phase characterized by a deep and relatively symmetric pressure minimum. For Qendresa, the selected time corresponds to the late mature phase, when the pressure minimum appears weaker and more asymmetric.

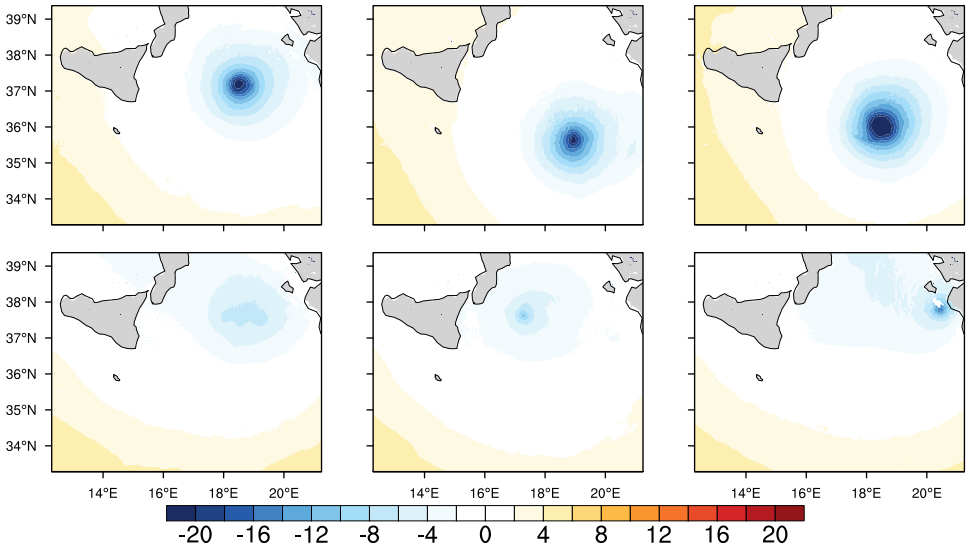

Figure 4. WRF surface pressure anomalies $\mathbf{P} - \langle \mathbf{P} \rangle$, where $\mathbf{P}$ is the pressure and $\langle \mathbf{P} \rangle$ is the average value of the pressure at a fixed isobaric level, in hPa, for Ianos (17 September 2020 06:00, **upper** panel) and Qendresa (8 November 2014 14:00, **lower** panel). Columns correspond to the three WRF configurations (S01, S02, S03).

3.3. Three-Dimensional Structure of Ianos

This subsection focuses on the three-dimensional structure of Ianos during its mature phase, analyzing wind and temperature fields at multiple pressure levels. The selected time step corresponds to a dynamically stable stage of the cyclone, identified based on the temporal evolution of $E_k(t)$ and $\epsilon(t)$ shown in Figure 3.

Figure 5 shows the wind speed fields at 1000, 850, and 500 hPa. The cyclone exhibits a compact and relatively symmetric structure, with well-organized wind maxima around the cyclone core and a gradual decrease of wind intensity with height. The persistence of a coherent circulation across the three levels highlights the vertically organized nature of the system during its mature stage.

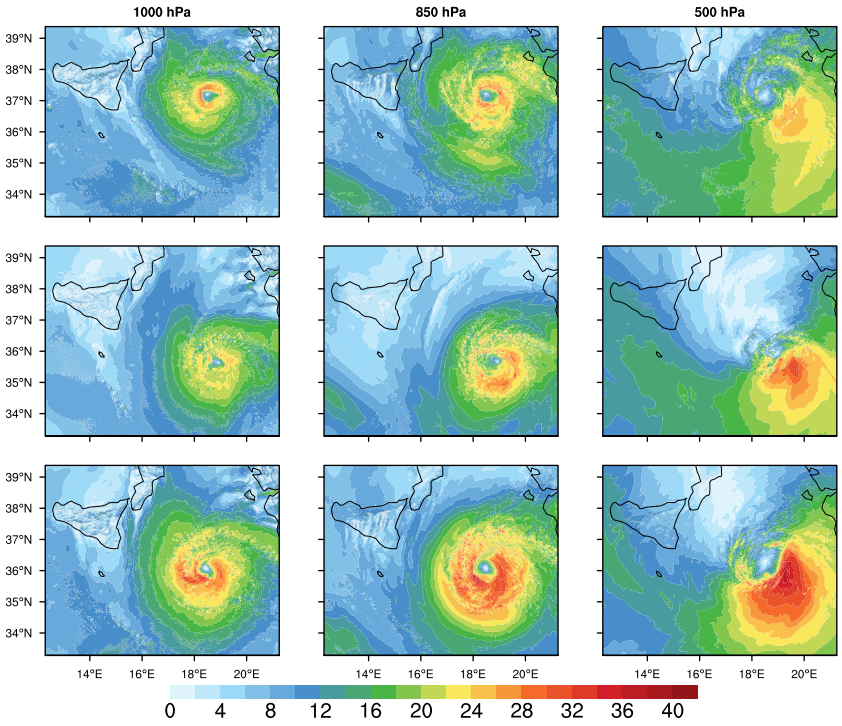

Figure 5. WRF wind speed (m s^{-1}) at the selected model time step (17 September 2020 06:00), during the mature phase of the Medicane Ianos. Rows correspond to the three WRF configurations (S01, S02, S03), while columns show the 1000, 850, and 500 hPa levels.

At 1000 hPa, the strongest winds are concentrated close to the cyclone center, while at 850 hPa, the circulation remains well defined and spatially coherent. At 500 hPa, although wind speeds are reduced, the cyclonic structure is still clearly identifiable, indicating a strong vertical continuity of the flow. This vertical consistency characterizes the structure of the cyclone at the selected time.

The wind speed anomalies shown in Figure 6 further emphasize the localized intensification of the circulation, particularly at low and mid-tropospheric levels. Positive anomalies are spatially coherent and organized around the cyclone core, indicating that departures from the mean flow are associated with persistent dynamical features rather than small-scale noise. The spatial organization of the anomalies suggests a stable inner-core structure in this phase.

Figure 7 displays the temperature anomalies at the same time step, revealing a well-defined warm core extending from 1000 to 500 hPa. The vertical extent and coherence of the positive temperature anomalies are consistent with a fully developed tropical-like structure. The presence of a vertically aligned warm core provides thermodynamic support to the organized wind field observed in Figures 5 and 6, confirming that the selected time step is representative of a mature and dynamically coherent phase of Ianos.

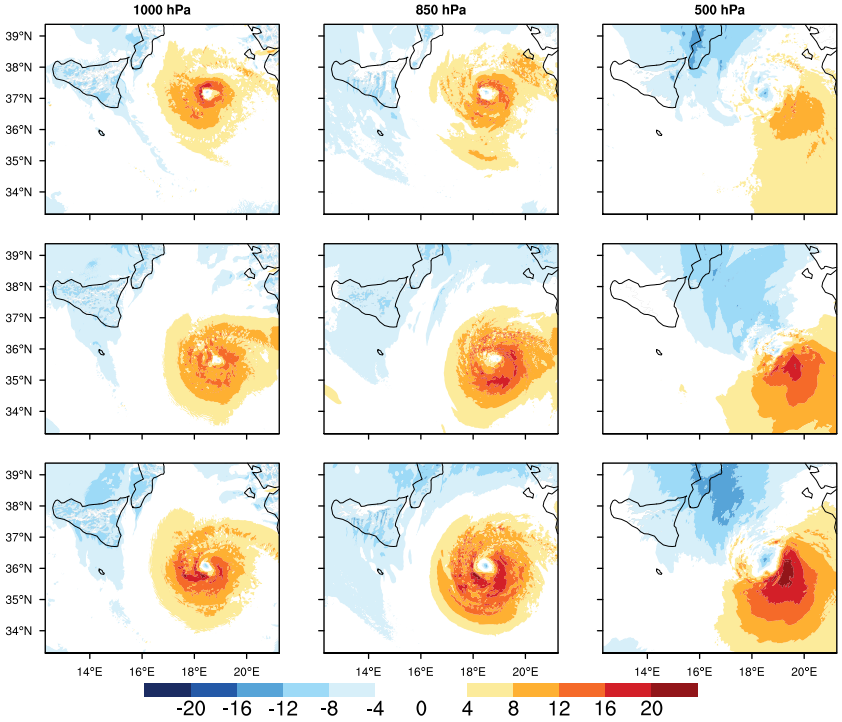

Figure 6. WRF wind speed anomalies $\mathbf{U} - \langle \mathbf{U} \rangle$, where $\mathbf{U}$ is the wind speed and $\langle \mathbf{U} \rangle$ is the average value of the wind speed at a fixed isobaric level, in m s^{-1}, at the selected model time step (17 September 2020 06:00), during the mature phase of the Medicane Ianos. Rows correspond to the three WRF configurations (S01, S02, S03), while columns show the 1000, 850, and 500 hPa levels.

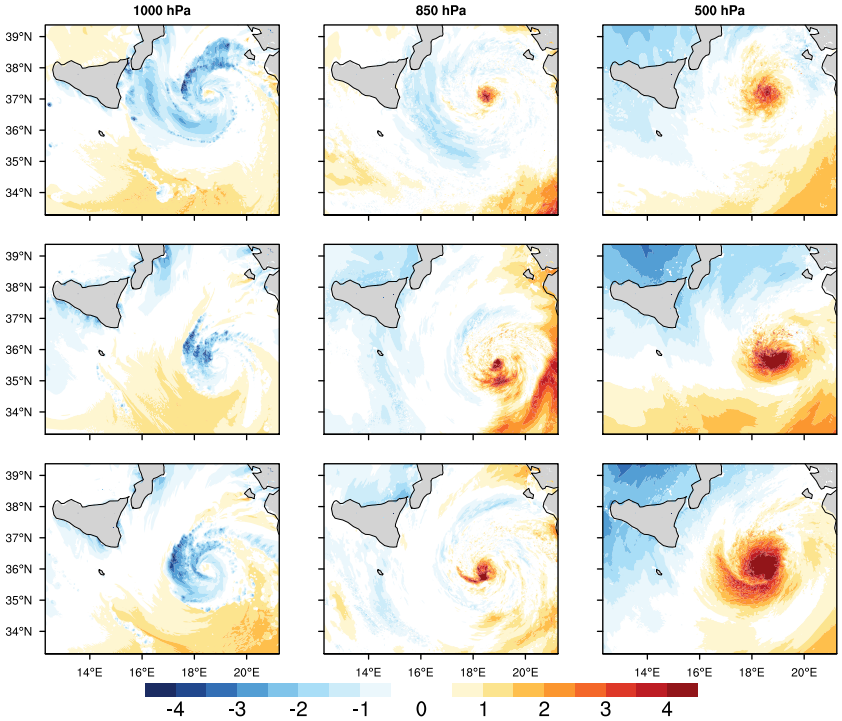

Figure 7. WRF temperature anomalies $\mathbf{T} - \langle \mathbf{T} \rangle$, where $\mathbf{T}$ is the temperature and $\langle \mathbf{T} \rangle$ is the average value of the temperature at a fixed isobaric level, in K, at the selected model time step (17 September 2020 06:00), during the mature phase of the Medicane Ianos. Rows correspond to the three WRF configurations (S01, S02, S03), while columns show the 1000, 850, and 500 hPa levels.

3.4. Three-Dimensional Structure of Qendresa

Following the same approach adopted for Ianos, the same set of variables is analyzed for Qendresa. The focus is on a late mature phase of the cyclone, selected to highlight structural differences with respect to Ianos and to illustrate the impact of a less stationary and more baroclinically influenced evolution.

Figure 8 shows the wind speed fields during this stage of the cyclone evolution. Compared to Ianos, the wind structure appears broader and more asymmetric, with wind maxima that are less concentrated around the cyclone center and a stronger imprint of the surrounding environmental flow. The circulation remains identifiable at all levels, but its spatial organization is less compact.

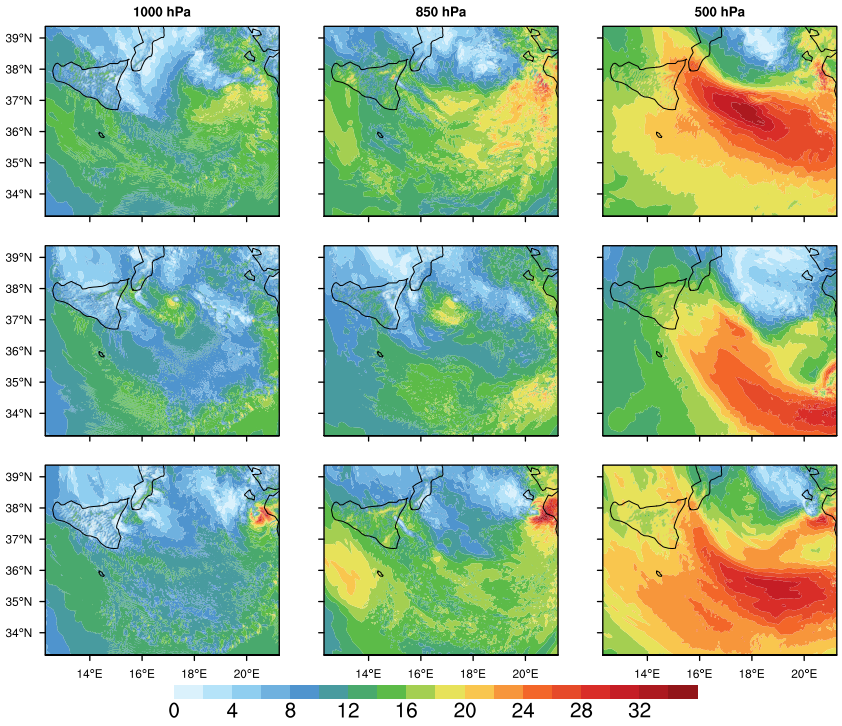

Figure 8. WRF wind speed (m s^{-1}) at the selected model time step (8 November 2014 14:00), during the late mature phase of the Medicane Qendresa. Rows correspond to the three WRF configurations (S01, S02, S03), while columns show the 1000, 850, and 500 hPa levels.

At 1000 hPa, the strongest winds are distributed over a wider area and are not as tightly clustered around the core as in Ianos. At 850 and 500 hPa, the cyclonic circulation becomes progressively less coherent, indicating a reduced vertical alignment of the flow. This reduced vertical coherence reflects a more complex and less consolidated structure during the selected phase of the cyclone.

The wind speed anomalies shown in Figure 9 exhibit fragmented and spatially heterogeneous patterns. Regions of positive and negative anomalies are distributed irregularly, with no clear symmetry around the cyclone center. This behavior indicates that departures from the mean flow are associated with transient and spatially variable features rather than with a persistent inner-core structure.

Figure 10 shows temperature anomalies characterized by weaker and more asymmetric patterns compared to Ianos. The warm core is less intense and less vertically extended, with positive anomalies confined to a smaller portion of the troposphere. The reduced vertical coherence of the thermal structure is consistent with the less organized wind fields observed in Figures 8 and 9, indicating that the selected time step represents a late mature phase in which the cyclone structure is already undergoing partial reorganization.

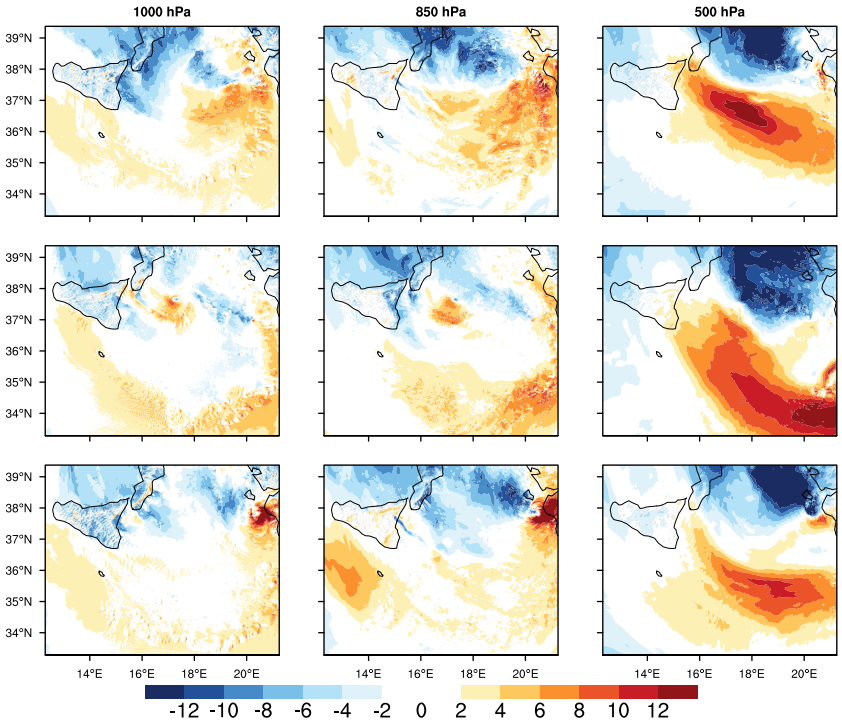

Figure 9. WRF wind speed anomalies $\mathbf{U} - \langle \mathbf{U} \rangle$, where $\mathbf{U}$ is the wind speed and $\langle \mathbf{U} \rangle$ is the average value of the wind speed at a fixed isobaric level, in m s^{-1}, at the selected model time step (8 November 2014 14:00), during the mature phase of the Medicane Qendresa. Rows correspond to the three WRF configurations (S01, S02, S03), while columns show the 1000, 850, and 500 hPa levels.

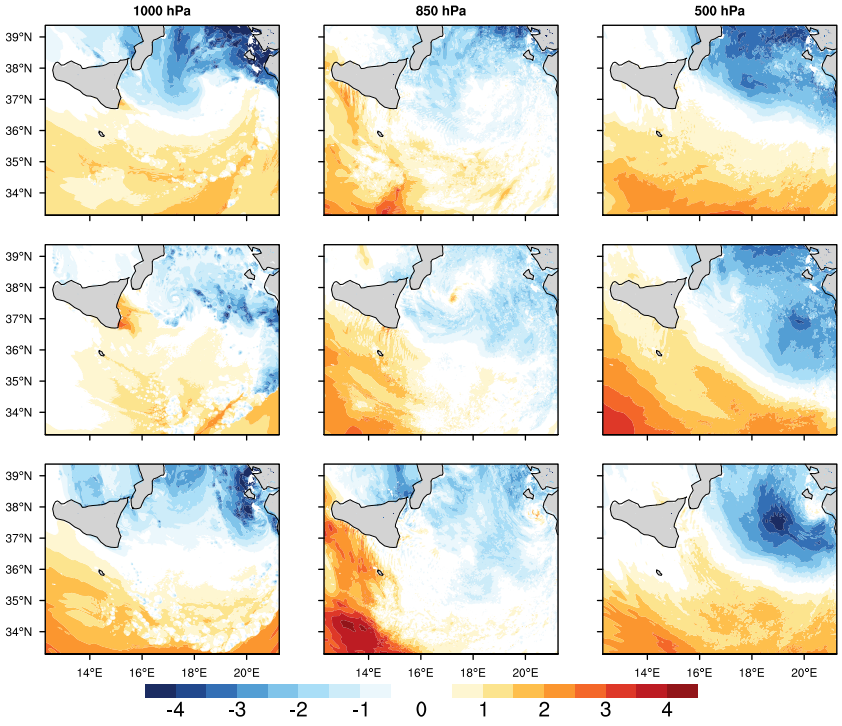

Figure 10. WRF temperature anomalies $\mathbf{T} - \langle \mathbf{T} \rangle$, where $\mathbf{T}$ is the temperature and $\langle \mathbf{T} \rangle$ is the average value of the temperature at a fixed isobaric level, in K, at the selected model time step (8 November 2014 14:00), during the mature phase of the Medicane Qendresa. Rows correspond to the three WRF configurations (S01, S02, S03), while columns show the 1000, 850, and 500 hPa levels.

3.5. WRF–ERA5 Comparison of MTLCs Intensity

To further contextualize the simulated cyclone structures, WRF results are compared with the ERA5 reanalysis in terms of cyclone intensity, focusing on MSLP and MWS. This comparison aims to assess systematic differences between high-resolution simulations (WRF) and a coarser-resolution large-scale reference (ERA5), providing insight into the representation of cyclone intensity across scales. These differences do not represent model errors with respect to observations, but quantify the relative behavior of WRF simulations within a consistent reference framework.

The WRF–ERA5 comparison highlights systematic differences in cyclone intensity metrics that depend on both the considered event and the model configuration (Table 3).

Table 3. WRF–ERA5 comparative metrics for minimum sea-level pressure (MSLP) and maximum 10-m wind speed (MWS).

Event	Run	MSLP (hPa)			MWS (m s^{-1})		
		MB	RMSE	MAE	MB	RMSE	MAE
Ianos	S01	−22.0	29.1	22.0	14.2	15.4	14.2
Ianos	S02	−12.3	23.3	15.6	3.5	6.9	5.6
Ianos	S03	−20.1	25.8	20.1	9.9	13.7	11.7
Qendresa	S01	−26.9	90.2	30.7	2.3	4.2	3.3
Qendresa	S02	−27.7	89.2	29.7	2.2	4.1	3.0
Qendresa	S03	−27.6	89.6	30.0	0.6	3.2	2.6

For Ianos, all WRF configurations exhibit a negative MB in MSLP and a positive MB in MWS, indicating that the simulated cyclone is characterized by lower central pressure values and stronger near-surface winds in WRF relative to ERA5. The magnitude of both bias and dispersion metrics varies across configurations, with S02 showing the smallest differences, while S01 and S03 display larger deviations.

For Qendresa, a negative MB in MSLP is also found across all configurations, with comparable magnitudes among S01–S03. However, RMSE values for MSLP are substantially larger than for Ianos, indicating a higher temporal variability in the WRF–ERA5 differences. In contrast, differences in MWS remain limited, with weak biases and low RMSE and MAE values across all configurations. This behaviour is consistent with the hybrid dynamical nature of MTLCs, in which baroclinic processes and air–sea interaction jointly contribute to the system evolution. As a consequence, different intensity metrics, including central pressure and maximum wind speed, may respond differently to the underlying physical processes [12,33,34].

Overall, the results indicate that WRF-ERA5 differences are event-dependent, with more systematic discrepancies for Ianos and more variable, pressure-dominated differences for Qendresa.

4. Discussion

This section provides a physical interpretation of the simulated structures and intensity metrics of Ianos and Qendresa from a modeling perspective. The focus is on how differences in dynamical regime, parameterization choices, and model resolution influence the representation of MTLCs in high-resolution simulations.

4.1. Modeling Perspective and Parameterizations

The differences documented in the Results for the various simulation configurations reflect the different dynamical regimes of the two MTLCs. For Ianos, the strong dynamical organization of the system tends to constrain the variability introduced by changes in

physical parameterizations, resulting in a quasi-stationary turbulent regime during the mature phase, consistent with tropical cyclones dominated by PBL coupling and surface fluxes [35].

In contrast, Qendresa exhibits a much higher sensitivity to parameterization choices. As a baroclinic-to-tropical transition system, its evolution is intrinsically less stationary, and the turbulent response is more strongly modulated by interactions with large-scale dynamics. This behavior is consistent with previous findings on turbulence in dynamically non-homogeneous and less predictable cyclones [36].

The enhanced variability observed in configurations S02 and S03 suggests that changes in microphysical and radiative representations directly influence the temporal structure of turbulent dissipation, particularly in systems dominated by baroclinic forcing, in agreement with studies on energy cascade processes and variability driven by large-scale dynamical interactions [37]. The comparison between Ianos and Qendresa further indicates that the sensitivity of turbulence to physical parameterizations increases in systems less dominated by deep convection and more influenced by baroclinic processes, highlighting the key role of the underlying dynamical structure and PBL processes [38].

It should be noted that part of the differences between the simulations may also reflect the intrinsic sensitivity of the model solution to small perturbations in the model configuration or initial state, which is a known characteristic of nonlinear atmospheric systems. A full assessment of this aspect would require ensemble simulations with perturbed initial conditions and/or model parameters, which are beyond the scope of the present work but will be addressed in future studies.

4.2. Comparison Between Ianos and Qendresa

This subsection provides a comparative interpretation of the three-dimensional structure of Ianos and Qendresa in terms of their underlying dynamical regimes.

The comparison between Ianos and Qendresa highlights how the simulated structure of MTLCs strongly depends on their underlying dynamical regime and evolutionary stage. For Ianos, the compact and vertically coherent wind and temperature structures reflect a mature, convection system, in which the coupling between PBL and free troposphere supports a well-organized inner-core circulation. In contrast, Qendresa exhibits a broader and more asymmetric structure, with reduced vertical coherence and a weaker warm core, consistent with a system still influenced by baroclinic forcing and large-scale environmental flow. These structural differences are consistent with the temporal behavior of $E_k(t)$ and $\epsilon(t)$ shown in Figure 3 and help explain the different patterns observed in the WRF-ERA5 intensity comparison. Overall, the results indicate that high-resolution simulations are able to reproduce markedly different three-dimensional organizations for cyclones with similar classifications but distinct dynamical pathways, underscoring the importance of accounting for the cyclone regime when interpreting high-resolution model outputs.

These differences remain recognizable across all tested model configurations, indicating that the inferred dynamical contrast is not an artefact of a specific parameterization choice, but a robust feature of the simulated cyclone evolution. These results are broadly consistent with previous studies on MTLCs, which emphasize the hybrid dynamical nature of these systems and the coexistence of baroclinic forcing and air–sea interaction processes [12,33,34]. In particular, the structural differences observed between the two events reflect the range of dynamical regimes that can characterize Medicanes. Therefore, rather than introducing a fundamentally different interpretation, the present analysis reinforces previous findings by providing a comparative modeling perspective on how these processes are represented in high-resolution simulations.

4.3. Interpretation of WRF-ERA5 Intensity Differences

The differences identified in the WRF-ERA5 comparison (Table 3) can be interpreted in light of both the intrinsic characteristics of the two cyclones and the different spatial scales represented by high-resolution simulations and global reanalyses. ERA5 provides a dynamically consistent large-scale reference, but its effective resolution limits the representation of sharp pressure gradients and compact inner-core structures associated with intense MTLCs [30].

For Ianos, a strongly convective and well-organized tropical-like cyclone, the persistent negative MSLP bias and positive MWS bias indicate that high-resolution WRF simulations tend to intensify the cyclone core relative to ERA5. This behavior is consistent with previous studies showing that high-resolution models more effectively represent localized deepening and strong near-surface winds associated with organized deep convection and warm-core development [15,35]. The relatively low RMSE values further suggest that these differences are systematic and maintained throughout the mature phase of the cyclone.

In contrast, Qendresa exhibits substantially larger RMSE values for MSLP despite comparable MBs across configurations. This reflects a more complex and less stationary evolution, characteristic of systems strongly influenced by large-scale baroclinic forcing and structural reorganization, in which the pressure field is particularly sensitive to timing differences [13,32]. In this context, discrepancies between WRF and ERA5 are amplified in time, even when the mean bias remains relatively constant. The comparatively small differences in MWS indicate that, for Qendresa, surface wind intensity is less directly linked to the depth of the pressure minimum than in Ianos, consistent with a stronger influence of large-scale baroclinic forcing.

Overall, these results demonstrate that WRF-ERA5 differences are strongly modulated by the dynamical regime of the cyclone. Convection-dominated systems tend to exhibit systematic intensification in high-resolution simulations relative to reanalysis products, whereas transitional or baroclinically influenced systems show larger temporal variability and less consistent intensity differences. This highlights the importance of interpreting reanalysis-based comparisons within the appropriate dynamical context, rather than as direct indicators of model performance.

5. Conclusions

This study investigated the structure and evolution of two MTLCs, Ianos (2020) and Qendresa (2014), using high-resolution WRF simulations within a physically consistent modeling framework. Although both events are classified as MTLCs, the results reveal substantial differences in their dynamical behavior and vertical organization.

Ianos exhibits a compact, vertically coherent and strongly convective structure, characterized by a pronounced warm core and a strong coupling between the PBL and the free troposphere. In contrast, Qendresa shows a broader and more asymmetric organization, reduced vertical coherence, and a stronger influence of large-scale baroclinic forcing, reflecting a less stationary and more complex dynamical evolution.

The analysis demonstrates that the combined examination of energetic diagnostics and vertical structure provides a useful framework for identifying the underlying dynamical regime of MTLCs. In particular, differences in the temporal evolution of $E_k(t)$ and $\epsilon(t)$ emerge as robust indicators distinguishing convection-dominated systems from cyclones more strongly influenced by baroclinic processes.

A key outcome of the study is that these dynamical contrasts remain evident across multiple physically plausible parameterization configurations. This indicates that the identified differences between the two cyclones are not primarily configuration-dependent but reflect robust regime-dependent behaviour. In this sense, the present work goes beyond

a case-by-case description and provides a modeling framework for discriminating between distinct dynamical pathways of MTLC evolution.

The comparison between high-resolution WRF simulations and the ERA5 reanalysis further shows that differences in simulated cyclone intensity depend on both the dynamical regime of the event and the spatial scales represented by the models. In particular, pressure and wind-based intensity metrics do not necessarily provide equivalent information in hybrid systems, where baroclinic forcing and air–sea interaction may affect different components of the vortex in different ways.

Overall, the results highlight the importance of accurately representing mesoscale dynamics, planetary boundary layer processes, and vertical structure when interpreting and modeling MTLCs in both numerical weather prediction and regional climate simulations over the Mediterranean region.

Future work will extend this analysis to a larger set of MTLCs in order to assess the robustness of the identified dynamical regimes across different environmental conditions and evolutionary pathways. Particular attention will be devoted to the turbulent properties of MTLCs and to the mechanisms governing the transfer of energy from large-scale circulation features to mesoscale and smaller-scale motions.

Author Contributions: Conceptualization, C.N.G. and F.C.; methodology, C.N.G. and F.C.; software, C.N.G. and F.C.; validation, C.N.G. and F.C.; formal analysis, C.N.G. and F.C.; investigation, C.N.G. and F.C.; resources, C.N.G. and F.C.; data curation, C.N.G. and F.C.; writing—original draft preparation, C.N.G. and F.C.; writing—review and editing, C.N.G. and F.C.; visualization, C.N.G. and F.C.; supervision, C.N.G. and F.C.; project administration, C.N.G. and F.C.; funding acquisition, C.N.G. and F.C. All authors have read and agreed to the published version of the manuscript.

Funding: Italian national research program Fondo per il Programma Nazionale di Ricerca e Progetti di Rilevante Interesse Nazionale (PRIN), under the project "TURBIMECs: study of TURBulence In MEditerranean Cyclone events", grant n. 2022S3RSCT, CUP Master B53D23007500006, funded by the Italian Ministry of University and Research (MUR).

Institutional Review Board Statement: Not applicable.

Informed Consent Statement: Not applicable.

Data Availability Statement: The ERA5 data used are available on the Copernicus Climate Change Service, Climate Data Store, (2023): ERA5 hourly data on single levels from 1940 to present. Copernicus Climate Change Service (C3S) Climate Data Store (CDS). https://doi.org/10.24381/cds.adbb2d47 (accessed on 22 January 2026). WRF data (wind velocity components, surface pressure, and temperature) are available on zenodo (https://doi.org/10.5281/zenodo.18506852). The other WRF data are available upon request.

Conflicts of Interest: The authors declare no conflicts of interest.

References

1. Miglietta, M.M.; Flaounas, E.; González-Alemán, J.J.; Panegrossi, G.; Gaertner, M.A.; Pantillon, F.; Pasquero, C.; Schultz, D.M.; D'Adderio, L.P.; Dafis, S.; et al. Defining Medicanes: Bridging the Knowledge Gap Between Tropical and Extratropical Cyclones in the Mediterranean. *Bull. Am. Meteorol. Soc.* **2025**, *106*, E1955–E1971. [CrossRef]
2. Michaelides, S.; Karacostas, T.; Sánchez, J.L.; Retalis, A.; Pytharoulis, I.; Homar, V.; Romero, R.; Zanis, P.; Giannakopoulos, C.; Bühl, J.; et al. Reviews and perspectives of high impact atmospheric processes in the Mediterranean. *Atmos. Res.* **2018**, *208*, 4–44. [CrossRef]
3. Nastos, P.; Papadimou, K.K.; Matsangouras, I. Mediterranean tropical-like cyclones: Impacts and composite daily means and anomalies of synoptic patterns. *Atmos. Res.* **2018**, *208*, 156–166. [CrossRef]
4. Giovannini, L.; Davolio, S.; Zaramella, M.; Zardi, D.; Borga, M. Multi-model convection-resolving simulations of the October 2018 Vaia storm over Northeastern Italy. *Atmos. Res.* **2021**, *253*, 105455. [CrossRef]

5. Patlakas, P.; Stathopoulos, C.; Tsalis, C.; Kallos, G. Wind and wave extremes associated with tropical-like cyclones in the Mediterranean basin. *Int. J. Climatol.* **2021**, *41*, E1623–E1644. [CrossRef]
6. Drobinski, P.; Ducrocq, V.; Alpert, P.; Anagnostou, E.; Béranger, K.; Borga, M.; Braud, I.; Chanzy, A.; Davolio, S.; Delrieu, G.; et al. HyMeX: A 10-year multidisciplinary program on the Mediterranean water cycle. *Bull. Am. Meteorol. Soc.* **2014**, *95*, 1063–1082. [CrossRef]
7. Miglietta, M.M.; Mastrangelo, D.; Conte, D. Influence of physics parameterization schemes on the simulation of a tropical-like cyclone in the Mediterranean Sea. *Atmos. Res.* **2015**, *153*, 360–375. [CrossRef]
8. IPCC. *Climate Change 2022: Impacts, Adaptation, and Vulnerability*; Cambridge University Press: Cambridge, UK; New York, NY, USA, 2022. [CrossRef]
9. Lazoglou, G.; Papadopoulos-Zachos, A.; Georgiades, P.; Zittis, G.; Velikou, K.; Manios, E.M.; Anagnostopoulou, C. Identification of climate change hotspots in the Mediterranean. *Sci. Rep.* **2024**, *14*, 29817. [CrossRef]
10. Romero, R.; Emanuel, K. Medicane risk in a changing climate. *J. Geophys. Res. Atmos.* **2013**, *118*, 5992–6001. [CrossRef]
11. Cavicchia, L.; von Storch, H.; Gualdi, S. Mediterranean tropical-like cyclones in present and future climate. *J. Clim.* **2014**, *27*, 7493–7501. [CrossRef]
12. Miglietta, M.M.; Rotunno, R. Development mechanisms for Mediterranean tropical-like cyclones (medicanes). *Q. J. R. Meteorol. Soc.* **2019**, *145*, 1444–1460. [CrossRef]
13. Flaounas, E.; Davolio, S.; Raveh-Rubin, S.; Pantillon, F.; Miglietta, M.M.; Gaertner, M.A.; Hatzaki, M.; Homar, V.; Khodayar, S.; Korres, G.; et al. Mediterranean cyclones: Current knowledge and open questions on dynamics, prediction, climatology and impacts. *Weather Clim. Dyn.* **2022**, *3*, 173–208. [CrossRef]
14. Moscatello, A.; Miglietta, M.M.; Rotunno, R. Numerical analysis of a Mediterranean "hurricane" over southeastern Italy. *Mon. Weather Rev.* **2008**, *136*, 4373–4397. [CrossRef]
15. Pantillon, F.; Davolio, S.; Avolio, E.; Calvo-Sancho, C.; Carrió, D.S.; Dafis, S.; Gentile, E.S.; Gonzalez-Aleman, J.J.; Gray, S.; Miglietta, M.M.; et al. The crucial representation of deep convection for the cyclogenesis of Medicane Ianos. *Weather Clim. Dyn.* **2024**, *5*, 1187–1205. [CrossRef]
16. Dafis, S.; Claud, C.; Kotroni, V.; Lagouvardos, K.; Rysman, J.F. Insights into the convective evolution of Mediterranean tropical-like cyclones. *Q. J. R. Meteorol. Soc.* **2020**, *146*, 4147–4169. [CrossRef]
17. Fernández-Alvarez, J.C.; Vázquez, M.; Pérez-Alarcón, A.; Nieto, R.; Gimeno, L. Comparison of moisture sources and sinks estimated with different versions of FLEXPART and FLEXPART-WRF models forced with ECMWF reanalysis data. *J. Hydrometeorol.* **2023**, *24*, 221–239. [CrossRef]
18. Chericoni, M.; Fosser, G.; Flaounas, E.; Sannino, G.; Anav, A. Extreme Mediterranean cyclones and associated variables in an atmosphere-only vs. an ocean-coupled regional model. *Weather Clim. Dyn.* **2025**, *6*, 627–643. [CrossRef]
19. Koseki, S.; Mooney, P.A.; Cabos, W.; Gaertner, M.Á.; de la Vara, A.; González-Alemán, J.J. Modelling a tropical-like cyclone in the Mediterranean Sea under present and warmer climate. *Nat. Hazards Earth Syst. Sci.* **2021**, *21*, 53–71. [CrossRef]
20. Skamarock, W.C.; Klemp, J.B.; Dudhia, J.; Gill, D.O.; Barker, D.M.; Duda, M.G.; Huang, X.Y.; Wang, W.; Powers, J.G. *A Description of the Advanced Research WRF Version 3*; NCAR Technical Note; National Center for Atmospheric Research: Boulder, CO, USA, 2008; NCAR/TN-475+STR.
21. Lagouvardos, K.; Karagiannidis, A.; Dafis, S.; Kalimeris, A.; Kotroni, V. Ianos—A hurricane in the Mediterranean. *Bull. Am. Meteorol. Soc.* **2022**, *103*, E1621–E1636. [CrossRef]
22. Mylonas, M.P.; Douvis, K.C.; Polychroni, I.D.; Politi, N.; Nastos, P.T. Analysis of a mediterranean tropical-like cyclone. Sensitivity to WRF parameterizations and horizontal resolution. *Atmosphere* **2019**, *10*, 425. [CrossRef]
23. Flaounas, E.; Aragão, L.; Bernini, L.; Dafis, S.; Doiteau, B.; Flocas, H.; Gray, S.L.; Karwat, A.; Kouroutzoglou, J.; Lionello, P.; et al. Composite Tracks of Mediterranean Cyclones (1979–2020). 2022. Available online: https://zenodo.org/records/7378600 (accessed on 22 January 2026).
24. NOAA . NCEP FNL Operational Model Global Tropospheric Analyses, Continuing from July 1999. 2000. Available online: https://gdex.ucar.edu/datasets/d083002/ (accessed on 22 January 2026).
25. Stull, R.B. *An Introduction to Boundary Layer Meteorology*; Springer Science & Business Media: Berlin/Heidelberg, Germany, 2012.
26. Garratt, J.R. The atmospheric boundary layer. *Earth-Sci. Rev.* **1994**, *37*, 89–134. [CrossRef]
27. Kaimal, J.C.; Finnigan, J.J. *Atmospheric Boundary Layer Flows: Their Structure and Measurement*; Oxford University Press: Oxford, UK, 1994.
28. Pope, S.B. Turbulent flows. *Meas. Sci. Technol.* **2001**, *12*, 2020–2021. [CrossRef]
29. Copernicus Climate Change Service (C3S). ERA5: Fifth Generation of ECMWF Atmospheric Reanalyses of the Global Climate. Copernicus Climate Data Store (CDS), 2017–Present. Available online: https://cds.climate.copernicus.eu (accessed on 22 January 2026).
30. Hersbach, H.; Bell, B.; Berrisford, P.; Hirahara, S.; Horányi, A.; Muñoz-Sabater, J.; Nicolas, J.; Peubey, C.; Radu, R.; Schepers, D. The ERA5 global reanalysis. *Q. J. R. Meteorol. Soc.* **2020**, *146*, 1999–2049. [CrossRef]

31. Pérez-Alarcón, A.; Coll-Hidalgo, P.; Trigo, R.M.; Nieto, R.; Gimeno, L. CyTRACK: An open-source and user-friendly python toolbox for detecting and tracking cyclones. *Environ. Model. Softw.* **2024**, *176*, 106027. [CrossRef]
32. Carrió, D.S. Improving the predictability of the Qendresa Medicane by the assimilation of conventional and atmospheric motion vector observations. Storm-scale analysis and short-range forecast. *Nat. Hazards Earth Syst. Sci.* **2023**, *23*, 847–869. [CrossRef]
33. Pytharoulis, I. Analysis of a Mediterranean tropical-like cyclone and its sensitivity to the sea surface temperatures. *Atmos. Res.* **2018**, *208*, 167–179. [CrossRef]
34. Gutiérrez-Fernández, J.; Miglietta, M.M.; González-Alemán, J.J.; Gaertner, M.A. A New Refinement of Mediterranean Tropical-Like Cyclones Characteristics. *Geophys. Res. Lett.* **2024**, *51*, e2023GL106429. [CrossRef]
35. Emanuel, K.; Velez-Pardo, M.; Cronin, T.W. The surprising roles of turbulence in tropical cyclone physics. *Atmosphere* **2023**, *14*, 1254. [CrossRef]
36. Kieu, C.; Rotunno, R. Characteristics of tropical-cyclone turbulence and intensity predictability. *Geophys. Res. Lett.* **2022**, *49*, e2021GL096544. [CrossRef]
37. Zhang, J.A. Spectral characteristics of turbulence in the hurricane boundary layer over the ocean between the outer rain bands. *Q. J. R. Meteorol. Soc.* **2010**, *136*, 918–926. [CrossRef]
38. Wang, S.; Tang, J. Analyzing coherent structures in the tropical cyclone boundary layer using large eddy simulations. *Trop. Cyclone Res. Rev.* **2024**, *13*, 230–238. [CrossRef]